Utility of Postoperative Magnetic Resonance Imaging in Patients Who Fail Superior Canal Dehiscence Surgery

Chemtob, Raphaelle A ; Epprecht, Lorenz ; Reinshagen, Katherine L ; Huber, Alexander ; Caye-Thomasen, Per ; Nakajima, Hideko H ; Lee, Daniel J

Abstract: OBJECTIVE: The etiology of symptoms following primary repair of superior canal dehiscence (SCD) may be due to a persistent third window. However, the extent of surgery cannot be seen on postoperative computed tomography (CT) since most repair materials are not radiopaque. We hypothesize that the extent of superior semicircular canal (SSC) occlusion following primary repair can be quantified based on postoperative magnetic resonance imaging (MRI) data. STUDY DESIGN: Retrospective series. SETTING: Tertiary care center. PATIENTS: Adult patients with a history of SCD syndrome who 1) report persistent symptoms following primary SCD repair and 2) underwent heavily T2-weighted MRI postoperatively. INTERVENTIONS: Analysis of SSC using 3D-reconstruction of CT co-registered with MRI data. MAIN OUTCOME MEASURES: Arc length of fluid void on MRI and quantification of persistent SCD based on CT/MRI co-registration. RESULTS: We identified 9 revision cases from a cohort of 145 SCD repairs at our institution (2002-2017) with CT/MRI data. A fluid void on postoperative MRI (indicating occlusion of the SSC) was observed in all cases (anterior limb: 50.1 degrees [±21.8 SD] and posterior limb 48.1 degrees [±28.5 SD]). Co-registration of CT/MRI revealed a residual defect that was most commonly found along the posterior limb in most patients with persistent symptoms. CONCLUSIONS: The extent of SCD repair can be determined using reformatted or direct T2-weighted MRI sequences in the plane of Pöschl. Co-registration of CT/MRI may be useful to determine the location of a residual superior canal defect and when present was found most commonly along the posterior limb.

DOI: https://doi.org/10.1097/mao.0000000000002051

Originally published at:
Chemtob, Raphaelle A; Epprecht, Lorenz; Reinshagen, Katherine L; Huber, Alexander; Caye-Thomasen, Per; Nakajima, Hideko H; Lee, Daniel J (2019). Utility of Postoperative Magnetic Resonance Imaging in Patients Who Fail Superior Canal Dehiscence Surgery. Otology Neurotology, 40(1):130-138.
DOI: https://doi.org/10.1097/mao.0000000000002051

Otology & Neurotology
xx:xx–xx © 2018, Otology & Neurotology, Inc.

Utility of Postoperative Magnetic Resonance Imaging in Patients Who Fail Superior Canal Dehiscence Surgery

*†‡§Raphaelle A. Chemtob, *†||Lorenz Epprecht, ¶Katherine L. Reinshagen, ||Alexander Huber, ‡Per Caye-Thomasen, *†Hideko H. Nakajima, and *†Daniel J. Lee

**Department of Otology and Laryngology, Massachusetts Eye and Ear, Harvard, Medical School; †Eaton Peabody Laboratories; ‡Department of Oto-Rhino-Laryngology, Head and Neck Surgery, and Audiology, Copenhagen University Hospital, Rigshospitalet; §Faculty of Health Sciences, University of Copenhagen, Copenhagen, Denmark; ||Department of Otorhinolaryngology, Head and Neck Surgery, University Hospital, Zurich, Switzerland; and ¶Department of Radiology, Massachusetts Eye and Ear, Boston, Massachusetts*

Objective: The etiology of symptoms following primary repair of superior canal dehiscence (SCD) may be due to a persistent third window. However, the extent of surgery cannot be seen on postoperative computed tomography (CT) since most repair materials are not radiopaque. We hypothesize that the extent of superior semicircular canal (SSC) occlusion following primary repair can be quantified based on postoperative magnetic resonance imaging (MRI) data.
Study design: Retrospective series.
Setting: Tertiary care center.
Patients: Adult patients with a history of SCD syndrome who 1) report persistent symptoms following primary SCD repair and 2) underwent heavily T2-weighted MRI postoperatively.
Interventions: Analysis of SSC using 3D-reconstruction of CT co-registered with MRI data.
Main outcome measures: Arc length of fluid void on MRI and quantification of persistent SCD based on CT/MRI co-registration.
Results: We identified 9 revision cases from a cohort of 145 SCD repairs at our institution (2002–2017) with CT/MRI data. A fluid void on postoperative MRI (indicating occlusion of the SSC) was observed in all cases (anterior limb: 50.1 degrees [±21.8 SD] and posterior limb 48.1 degrees [±28.5 SD]). Co-registration of CT/MRI revealed a residual defect that was most commonly found along the posterior limb in most patients with persistent symptoms.
Conclusions: The extent of SCD repair can be determined using reformatted or direct T2-weighted MRI sequences in the plane of Pöschl. Co-registration of CT/MRI may be useful to determine the location of a residual superior canal defect and when present was found most commonly along the posterior limb. **Key Words:** 3D reconstruction—Co-registration—Computed tomography—Magnetic resonance imaging—Middle fossa craniotomy—Revision surgery—Superior canal dehiscence—Transmastoid.

Otol Neurotol **39:**xxx–xxx, 2018.

As first reported by Minor et al. (1) in 1998, superior canal dehiscence (SCD) is a clinical syndrome associated with a bony defect of the superior semicircular canal (SSC). The dehiscence creates a third window of the inner ear and can result in a variety of auditory and/or vestibular complaints. In patients with debilitating symptoms, improvement can be achieved through closure of the third window and partial restoration of normal inner ear physiology (2). Persistence of symptoms after primary repair is uncommon with the plugging technique, but is felt to be due to incomplete occlusion of the defect or displacement of the repair material following surgery (3). Although patients who undergo revision surgery for SCD can do well postoperatively, the success rates are lower than in primary surgery and the risk of vestibular dysfunction and sensorineural hearing loss increases (4,5).

To facilitate the diagnosis of a persistent defect at the SCD repair site as the cause of symptoms, an accurate methodology to determine the extent of the initial repair must be used. Preoperative high resolution computed tomography (CT) is the gold standard to visualize the size and location of the SCD as well as surrounding skull base topography before repair (6). Postoperative CT scans can highlight the use of bone chips or bone cement to reconstruct the tegmen or fill the SSC defect but are not useful for the majority of SCD surgeries that are performed in the United States. This is because repair materials used by most surgeons (such as bone wax, fascia, and cartilage) are not radiopaque. This issue also applies to cases involving SCD ‘‘resurfacing’’ where

Address correspondence and reprint requests to Daniel J. Lee, M.D., F.A.C.S., Department of Otology and Laryngology, Massachusetts Eye and Ear, Harvard Medical School, 243 Charles Street, 02114 Boston, MA; E-mail: daniel_lee@meei.harvard.edu
Funding source: Oticon Fonden.
The authors disclose no conflicts of interest.
DOI: 10.1097/MAO.0000000000002051

materials such as cartilage and perichondrium are used. Creating a watertight seal using a ''cap'' over an arcuate eminence defect is more likely achieved through partial occlusion rather than ''resurfacing'' of the canal lumen at the defect and this is supported by postoperative imaging (Lee et al., unpublished data). In contrast, high resolution magnetic resonance imaging (MRI) reformatted to the Pöschl plane can highlight the remaining fluid signal in the superior canal and therefore provide an indirect measure of canal occlusion.

In this study, we hypothesize that the extent of SSC occlusion following primary repair can be quantified by the arc length of the fluid void on postoperative heavily T2-weighted MRI. Furthermore, co-registration and three-dimensional (3D) reconstruction of 1) the bony defect on preoperative CT combined with 2) postoperative heavily T2-weighted MRI sequences can determine whether there is incomplete repair of the SCD. Localizing a residual defect of the superior canal using both CT and MRI in the plane of Pöschl can serve as an anatomical guide for revision surgery.

METHODS

We performed a retrospective review of patients undergoing revision surgery for SCD syndrome between January 1st, 2002 and December 31st, 2017 at our institution. All patients initially presented with signs and symptom of SCD, the finding of a bony defect of the superior canal on high resolution CT, and audiometric testing and cervical vestibular-evoked myogenic potentials that suggested a physiologic change of the inner ear associated with the dehiscence. Inclusion criteria were 1) adults ($\geq$18 years old) with persistent symptoms following primary SCD repair and 2) patients with signs of a persistent ''third mobile window'' on audiometric and/or vestibular testing following primary SCD repair. Patients who had postoperative high resolution heavily T2-weighted MRI obtained postoperatively were included in the study. We included a control group of patients with complete resolution of symptoms following primary SCD repair and postoperative heavily T2-weighted MRI. Our main outcome measure was the extent of SSC occlusion following primary repair determined by the arc length of the fluid void on postoperative MRI data. Furthermore, the location of a residual defect at the SCD repair site was quantified in a co-registered 3D reconstruction of preoperative CT and postoperative MRI imaging.

The 3D-reconstruction of preoperative CT co-registered with postoperative MRI data was reviewed by two blinded authors (K.R., D.J.L.). Following the blinded analysis, the authors (K.R., D.J.L.) measured the fluid void on MRI and the bony defect on CT.

The study was approved by our Human Studies Committee (HSC #13-005H).

2D Reconstruction

High resolution CT images of the temporal bone were performed with 120 kVp, 240 mA, slice thickness of 0.6 mm and a 0.2 mm gap (Discovery 750 HD, General Electric, Milwaukee, WI). If accessible we used cone beam CT for the reconstruction images. Cone beam CT of the temporal bone was performed with 90 kVp, 8 mA, hi-resolution mode with a slice thickness of 0.5 mm (3D Accuitomo, J. Morito MFG Corp, Kyoto, Japan). High resolution heavily T2-weighted fast recovery turbo spin echo cisternographic MRI sequences of the temporal bone were performed (axial T2 3D DRIVE, Philips, the Netherlands). The imaging acquisition parameters were set as following: repetition time (TR): 1700 ms, echo time (TE): 190 ms, number of excitations (NEX): 3, slice thickness: 1 mm, spacing (SP): 0.5 mm, matrix: 412×337, scan time: 4 minutes and 37 seconds. An 8-channel head coil was used.

Preoperative and postoperative images were retrieved and imported into an imaging viewer software (OsiriX Lite 9.0, Pixmeo SARL, Bernex, Switzerland). In patients who did not have direct Pöschl, MRI and CT sequences were reformatted in the plane perpendicular to the long axis of the temporal bone (Pöschl view) before co-registered in a 2D plane. A demonstration of this 2D reconstruction is shown in Figures 1 and 2.

Postoperative MRI

The arc length of the fluid void in the SSC was measured on the postoperative heavily T2-weighted MRI sequences (DRIVE) of the temporal bone in the Pöschl reformat. A plane bisecting the inferior limb of the posterior semicircular canal was created extending through the apex of the SSC. The radius of the SSC was calculated and an angle was measured from the center of the SSC and along the plane of the bisected posterior semicircular canal/apex of the SSC, towards the fluid signal in the anterior limb. A second angle was measured towards the posterior limb of the SSC.

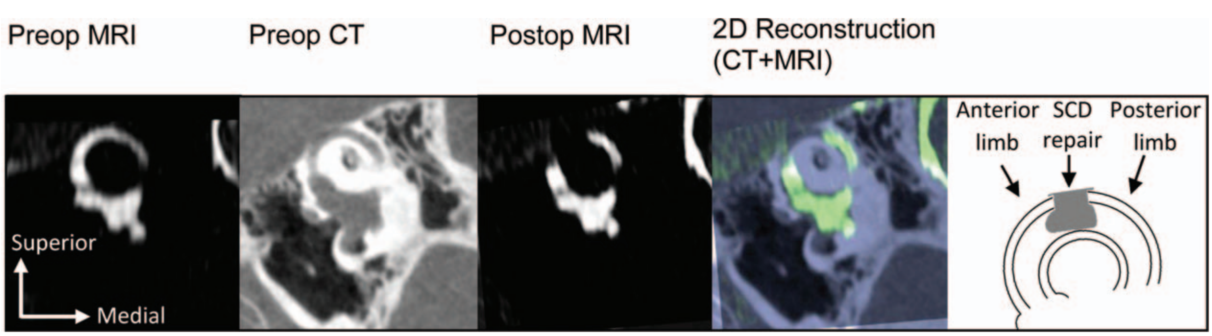

FIG. 1. Schematic and CT/MRI images of the superior semicircular canal (reformatted to the Pöschl plane). 57-year-old woman with left ear SCD following SSC plugging via MFC. Complete occlusion of the bony defect is seen on the CT+MRI overlay with symptom control. The MRI signal reflects the fluid in the SSC, which stops within the bony covering of the SSC and before the bony dehiscence, suggesting that the SSC is successfully plugged.

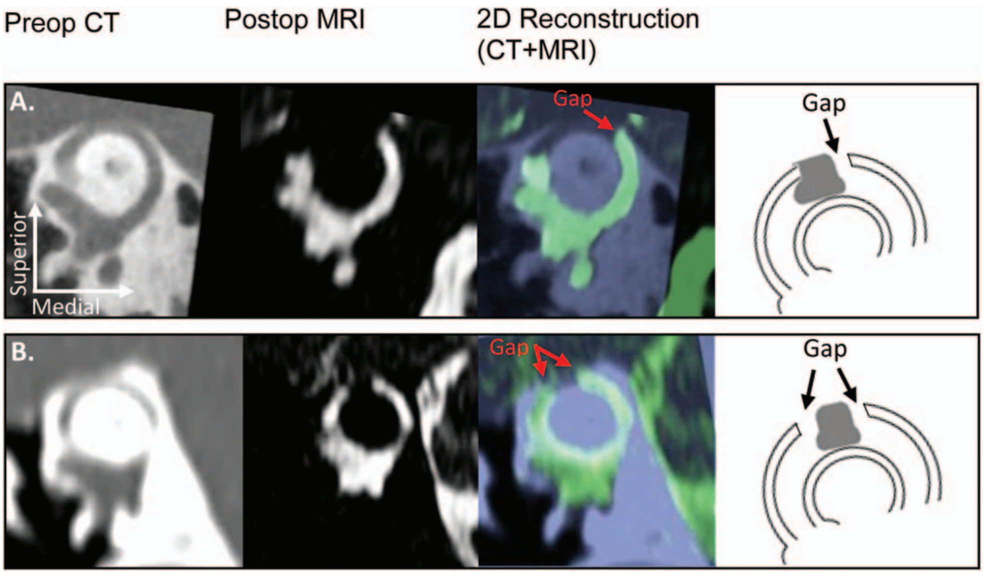

FIG. 2. Schematic and CT/MRI images of the superior semicircular canal (reformatted to the Pöschl plane). Patient A: 33-year-old man with left ear SCD following SSC plugging via MFC. A persistent defect at the SCD repair site at the posterior limb is seen on the CT+MRI overlay. This patient reported partial symptom relief of pulsatile tinnitus and hyperacusis but persistence of autophony. There were no complaints of dizziness or vertigo following surgery. Patient B: 60-year-old woman with right ear SCD following SSC plugging via MFC. A gap between the repair and SCD is observed along the anterior and posterior limbs on CT+MRI overlay. The patient reported improvement of autophony and dizziness or vertigo induced by straining (Hennebert's sign) but continued to experience pulsatile tinnitus. The MRI signal reflects the fluid in the SSC. The *arrows* points at the posterior and/or the anterior limb of the SSC, where the fluid seems to be going beyond the bony covering, suggestive of a persistent arcuate eminence defect. CT indicates computed tomography; MRI, magnetic resonance imaging; SCD, superior canal dehiscence; SSC, superior semicircular canal.

3D Reconstruction

Heavily T2-weighted MRI sequences (DRIVE) were imported into segmentation software (Slicer.org, version 4.8). For each patient, CT images (taken before primary surgery) were registered to the postoperative MRI images by manual landmark registration (Fig. 3). The remaining fluid signal in the SSC (from where the canal was not plugged) was segmented and transformed into a 3D model. The surrounding temporal bone was volume rendered. The 3D model of the remaining SSC fluid signal and the volume rendered temporal bone showing the bony defect were displayed in 3D mode. The size and location of any residual defect after primary surgery was assessed by comparing the fluid void on MRI in the SSC (an indirect measure of the plugged canal) with the bony defect as measured on CT. An example of a 3D reconstruction showing a persistent defect of the posterior limb of the SSC is seen in Figure 4. The arrows point to the fluid at the posterior limb that protrudes from the SSC (at the edge of the

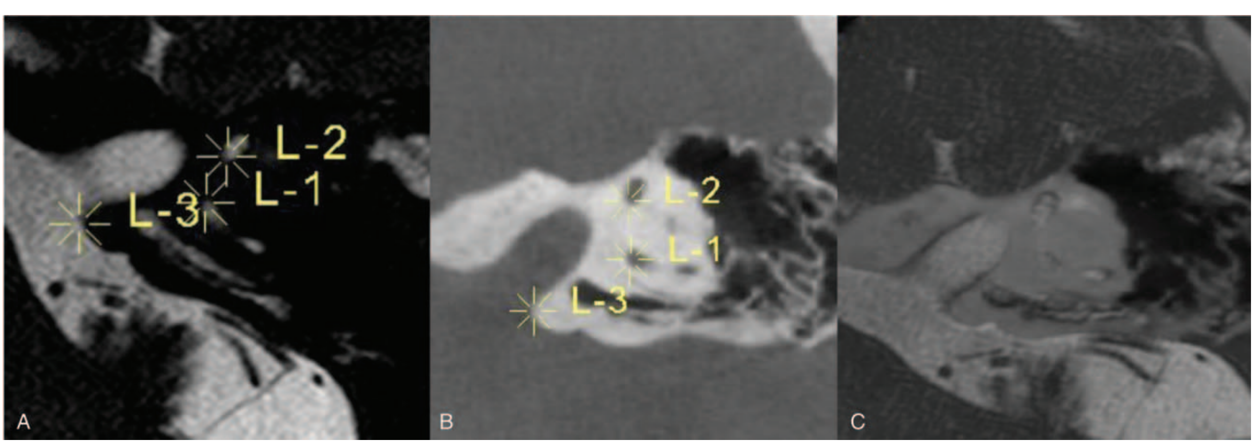

FIG. 3. Affine landmark registration of MRI and CT, left ear, axial plane. This is a 57-year-old woman with left ear SCD following SSC plugging via MFC. *A*, T2-weighted MRI with landmark registrations at posterior limb of SCC/common crus (L-1), anterior limb of SCC (L-2), and posterior lip of the porus acusticus (L-3). *B*, T2-weighted CT with similar landmark registrations. *C*, Composite image of A+B. CT indicates computed tomography; MRI, magnetic resonance imaging; SCD, superior canal dehiscence; SSC, superior semicircular canal.

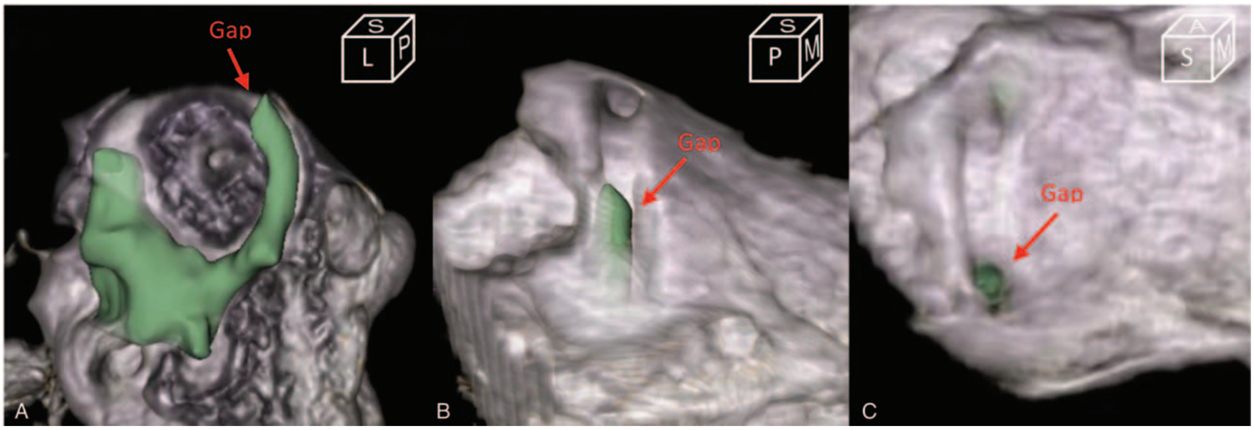

FIG. 4. Combined 3D reconstruction of CT and MRI imaging following SCD repair. 33-year-old man with left ear SCD following SSC plugging via MFC (same patient as in Fig. 2 [patient B]). A residual defect is noted in the posterior limb on combined 3D reconstruction of CT and MRI imaging. T2-weighted MRI signal represents the fluid in the SSC with the surrounding bony CT. *A*, parallel view of SSC (Pöschl view). *B*, posterior–superior view of SSC. *C*, Superior view of SSC. A indicates anterior; CT, computed tomography; L, lateral; M, medial; MRI, magnetic resonance imaging; P, posterior; S, superior; SCD, superior canal dehiscence; SSC, superior semicircular canal.

dehiscence). The anterior limb shows the fluid within the bony otic capsule of the SSC due to the plugging material successfully sealing the fluid.

RESULTS

We identified 17 revision cases from a cohort of 145 surgical SCD patients at our institution. A total of nine revision cases were identified that had high resolution heavily T2-weighted MRI imaging following primary surgical repair and were included in the study. From these patients, 4/9 had undergone initial SCD surgery at an outside institution. 7/9 patients had revision surgery, which were all at our institution. A total of four cases with complete resolution of symptoms postoperative were included as a control group. All four patients had undergone primary SCD surgery at our institution.

Patient characteristics are presented in Table 1.

In the study group, the majority of patients were women (56%) and most had left SCD (67%). Primary surgery was performed by middle fossa craniotomy in eight patients (89%), followed by a transmastoid approach in one patient due to a prominent superior petrosal sinus associated with a defect of the medial limb of the SSC (11%). All revision surgeries were performed by a transmastoid approach, as a revision craniotomy was not feasible in patients who had undergone primary surgery with a middle fossa craniotomy. The residual symptoms following primary surgery included both auditory (autophony, pulsatile tinnitus, hyperacusis) and vestibular complaints (chronic disequilibrium, sound, and/or pressure induced vertigo). Following revision surgery, all patients experienced improvement of symptoms. In the control group, the majority of patients were men (75%) and most had left SCD (75%). All patients underwent primary surgery with plugging of the SSC by middle fossa craniotomy. Pre- and postoperative audiometric and vestibular testing data are presented in Tables 2 and 3.

A fluid void on MRI (indicating occlusion of the SSC) following primary SCD repair was observed in all study and control patients (mean size of fluid void on the anterior 50.1 [±21.8 SD] versus 49.0 [±14.4 SD] degrees and posterior limb 48.1 [±28.5 SD] versus 68.2 [±28.6 SD]), respectively (Tables 4 and 5). A total of six of nine patients in the study group and one of four patients in the control group had a residual defect when comparing the arc length of the fluid void with the bony defect on CT (analysis No. 1, Table 4). This in comparison with the second analysis that deemed a residual defect in four of eight patients in the study group and zero of four patients in the control group.

The 3D-reconstruction of preoperative CT co-registered with postoperative MRI data was analyzed by two blinded authors (Tables 4 and 5). The first analysis suggested a residual defect in eight of nine patients in the study group and three of four patients in the control group (analysis No. 1). The second analysis suggested a residual defect in five of seven patients in the study group and one of four patients in the control group. Most persistent defects after primary repair were found posteriorly (towards the common crus) (6/11, 54%) (analysis No. 1) or both posteriorly and anteriorly (towards the ampulla) (3/6, 50%) (analysis No. 2, Table 5). The location of the defects was consistent between the two analyses (Tables 4 and 5).

DISCUSSION

The extent of the SSC occlusion following primary repair could be quantified based on postoperative heavily T2-weighted MRI. In most SCD patients with persistent symptoms after primary surgery, a residual defect at the surgical repair site could be identified when combining 3D reconstruction of the CT and MRI of the superior

TABLE 1. *Patient characteristics*

ID	Gender	Age	SCD Side	SCD Location	Primary Repair	Surgical Technique (Primary)	Residual Symptom	Revision Repair	Surgical Technique (Revision)	Persistent SCD Location	Improvement of Residual Symptom
Study group											
1	F	42	R	SPS	TM	Plugging, bone wax	Hennebert's, disequilibrium	TM	Plugging, bone wax	Posterior	Yes
2	F	50	L	AE	MFC	Plugging, bone wax	Autophony, hyperacusis, pulsatile tinnitus	TM	Plugging, bone wax	Posterior	Yes
3	F	54	L	AE	MFC	Plugging, bone wax	Autophony	TM	Plugging, bone wax, bone pate	Anterior	Yes
4	M	75	L	AE	MFC	Plugging, bone wax	Hyperacusis	TM	Plugging, bone wax, bone pate	Posterior	Yes
5	M	54	L	AE	MFC	Plugging, bone wax	Autophony, hyperacusis Hennebert's, Tulio	TM	Plugging, bone wax	Posterior, anterior	Yes
6	F	87	R	AE	MFC	Plugging, bone wax	Pulsatile tinnitus	N/A	N/A	No dehiscence seen	N/A
7	F	59	R	AE	MFC	Plugging, bone wax	Pulsatile tinnitus	TM	Plugging, bone wax	Posterior, anterior	Yes
8	M	49	L	AE	MFC	Plugging, bone wax	Pulsatile tinnitus, hyperacusis, disequilibrium	N/A	N/A	Posterior, anterior	N/A
9	M	33	L	AE	MFC	Plugging, bone wax	Autophony	TM	Plugging, bone wax	Posterior	Improvement of hyperacusis but persistent autophony
Control group											
10	F	57	L	AE	MFC	Plugging, bone wax	None	None			
11	M	54	R	AE	MFC	Plugging, bone wax	None	None			
12	M	37	L	AE	MFC	Plugging, bone wax	None	None			
13	M	33	L	AE	TM	Plugging, bone wax	None	None			

Majority of patients were men (54%) with left-sided SCD (69%). Most patients had a defect of the arcuate eminence of the SSC (as opposed to a bony defect of the descending limb of the superior canal from the superior petrosal sinus) and underwent MFC (92%). The SSC was plugged using bone wax in all cases.

TABLE 2. *Audiometric data before primary repair, after primary repair (before revision surgery) and after revision surgery*

	SCD Side	ABG 250 Hz Preop	ABG 500 Hz Preop	ABG 250 Hz Postop (Before Revision)	ABG 500 Hz Postop (Before Revision)	ABG 250 Hz Postop Revision	ABG 500 Hz Postop Revision
Study group							
1	Right	0	5	25	20	20	20
2	Left	25	10	30	5	25	5
3	Left	35	15	0	0	5	0
4	Left	25	15	0	0	25	5
5	Left	N/A	N/A	25	25	N/A	N/A
6	Right	40	35	30	30	N/A	N/A
7	Right	55	45	5	5	N/A	N/A
8	Left	10	10	10	5	N/A	N/A
9	Left	10	5	0	5	N/A	N/A
Control group							
10	Left	10	0	5	0		
11	Right	35	20				
12	Left	25	20	0	−5		
13	Left	10	5	15	0		

At baseline, all except one patient had an ABG on preoperative audiogram. Following primary SCD repair, four of eight patients had a decrease, two of eight patients had an increase and two of eight patients had no change in ABG in the study group. In the control group, one patient had a decrease and two of three patients had no change in ABG after primary repair. Following revision surgery, two of four patients had a continuous ABG, one patient had a continuous closure of ABG and one patients had an increase in ABG in the study group.

canal. In the majority of the cases, the residual defects after plugging were found posteriorly.

Imaging plays a crucial role in the diagnosis of SCD. CT scans with 0.5 mm collimation and reformatted in the planes of Pöschl (parallel to SSC) and Stenvers (orthogonal to SSC) are essential for diagnosing SCD (7). High resolution 3D imaging with cone beam CT can further improve the detection of SCD, but is not readily available in most centers (8). The absolute threshold of radiodensity above which intact bone can be predicted has not yet been established and consequently CT imaging can still overcall a dehiscence (9,10).

The goal of SCD surgery is to create a watertight seal and this is most reliably achieved by occluding the dehiscent canal. Resurfacing approaches are associated with a higher recurrence of symptoms. The extent of SSC repair in patients with persistent symptoms after primary SCD surgery, however, is difficult to assess as most repair materials are not radiopaque. In these cases, heavily T2 weighted MRI sequences (e.g., DRIVE, FIESTA, CISS) are useful in assessing the presence of fluid in the SSC following surgery. A fluid void in the superior canal is an indirect measure of the extent of repair. A postoperative MRI is also useful to exclude other culprits that explain persistent symptoms, such as fluid in the middle ear and mastoid, vascular malformations, tumors, or encephaloceles (3,11). In this study, we co-registered 3D reconstruction of CT and MRI imaging to determine the extent of SCD occlusion relative to the bony defect after primary surgical repair. Importantly, these data inform the clinician on the location and size of the residual defect that may explain persistent SCD symptoms and guide revision surgical repair, if indicated.

Lower rates of symptom improvement have been reported following revision surgery in comparison to primary repair (3). Therefore, careful selection of patients for revision surgery is important. This underscores the importance of a reliable means of determining a residual defect following SCD repair. Currently, the diagnosis of a persistent defect at the SCD repair site is based on patient symptomatology, auditory and vestibular testing (including cervical and/or ocular vestibular evoked myogenic potentials), and CT or MRI evidence of a persistent defect. Combined reconstruction of the superior canal using both CT and MRI can further improve preoperative assessment as previously shown in other types of surgery where soft tissue, cerebrospinal fluid, and bone are in close relationship. A previous study demonstrated the utility of 3D reconstruction using CT and MRI for the evaluation of tumors of the spine in patients with Neurofibromatosis type I. The combination of these imaging modalities improved visualization of bony abnormalities in relation to tumor morphology both pre- and postoperatively (12).

This study is the first to our knowledge to suggest this approach for the delineation of the SSC in patients who have undergone SCD surgery. Our imaging approach allowed for visualization of SCD repair and the location of residual defects. Measurements of the fluid void on MRI and the bony defect on CT suggested successful plugging of the SSC in all control patients (except one in analysis No. 1). More residual defects in the control group were found on 3D reconstruction. In the process of volume rendering, a threshold is chosen to distinguish the bone and the surrounding tissue and therefore this technique may overestimate the presence of a persistent defect. Co-registration of CT/MRI data was useful in determining the location of a residual defect in patients with symptoms but needs to be combined with arc length measurements in 2D to detect a defect.

TABLE 3. *cVEMP threshold data before primary repair, after primary repair (before revision surgery) and after revision surgery*

	SCD Side	cVEMP 250 Hz Preop	cVEMP 500 Hz Preop	cVEMP 750 Hz Preop	cVEMP 100 Hz Preop	cVEMP 250 Hz Postop (Before Revision)	cVEMP 500 Hz Postop (Before Revision)	cVEMP 750 Hz Postop (Before Revision)	cVEMP 1000 Hz Postop (Before Revision)	cVEMP 250 Hz Postop Revision	cVEMP 500 Hz Postop Revision	cVEMP 750 Hz Postop Revision	cVEMP 1000 Hz Postop Revision
Study group													
1	Right	75	90	90	95	100	100	N/A	N/A	90	100	100	100
2	Left	85	80	75	75	80	80	85	80	80	75	75	80
3	Left	35	35	45	55	65	60	70	80	90	80	80	80
4	Left	55	70	65	70	65	75	75	70	90	100	95	85
5	Left	N/A	N/A	N/A	N/A	50	55	55	65	N/A	N/A	N/A	N/A
6	Right	N/A	N/A	N/A	N/A	N/A	100	100	100	N/A	N/A	N/A	N/A
7	Right	90	85	90	90	N/A	90	95	100	N/A	90	85	100
8	Left	N/A	65	60	60	N/A	70	75	80	N/A	N/A	N/A	N/A
9	Left	N/A	N/A	N/A	N/A	65	60	N/A	70	N/A	70	80	85
Control group													
10	Left	N/A	65	60	65	N/A	75	80	85				
11	Right	60	65	75	75								
12	Left	N/A	60	60	70	N/A	85	90	90				
13	Left	65	60	N/A	70	N/A	95	95	95				

At baseline, seven of 10 patients had low cVEMP thresholds according to the guideline at our institution. Following primary SCD repair, all patients with available cVEMP data had an increase in thresholds of at least 10 dB HL in both the study (6/6) and control group (3/3). Following revision surgery, five of six patients had an addition increase and one patient had a decrease in cVEMP thresholds of at least 10 dB HL in the study group.

cVEMP indicates cervical vestibular evoked myogenic potentials.

TABLE 4. *Arc length measurements of the fluid void on postoperative MRI, the bony defect on preoperative CT, and 3D reconstruction of co-registration of CT/MRI*

ID	MRI Ant	MRI Post	CT Ant	CT Post	Anterior Limb	Posterior Limb	3D Ant	3D Post
Analysis No. 1								
Study group								
1	66	47	0	73	Plugged	Defect	Plugged	Defect
2	71	26	28	35	Plugged	Defect	Plugged	Defect
3	76	74	55	27	Plugged	Plugged	Defect	
4	19	45	62	44	Defect		Defect	Defect
5	11	18	24	41	Defect	Defect	Defect	Defect
6	78	77	33	53	Plugged	Plugged	Plugged	Plugged
7	20	14	28	17	Defect	Defect	Defect	Defect
8	12	31	8	43	Plugged	Defect	Plugged	Defect
9	64	41	22	29	Plugged	Plugged	Plugged	Defect
Control group								
10	35	38	11	41	Defect	Plugged	Defect	Plugged
11	58	69	22	29	Plugged	Plugged	Plugged	Plugged
12	33	99	27	33	Plugged	Plugged	Plugged	Defect
13	54	103	22	29	Plugged	Plugged	Plugged	Defect

A fluid void (indicating the extent of occlusion of the SSC) following primary repair was seen in all 13 cases. A total of six of nine patients in the study group and one of four patients in the control group had a residual defect when comparing the fluid void with the bony defect on the preoperative CT. The 3D reconstruction suggested a residual defect in eight of nine patients in the study group and three of four patients in the control group. CT indicates computed tomography; MRI, magnetic resonance imaging.

Our results showed that the majority of persistent defects after plugging were found posteriorly. An example is shown in Figure 4, where the 3D reconstruction revealed a remaining defect of the posterior limb. During middle fossa craniotomy, the anterior limb of the SCC is closest to the surgeon and occlusion is more easily achieved towards the ampulla. The posterior limb is further away and can be difficult to reach, especially in cases where the tegmen is downsloping away from the surgeon (6,13). Similarly, during transmastoid repair the anterior limb is also closest to the surgeon and is easier to access and repair compared with the posterior limb. Based on our observations we think that the nonampullated limb of the superior canal is at greater risk for a residual defect following surgery.

The goal of SCD surgery is to achieve a sufficient fluid seal without compromising the ampulla or common crus. Excessive occlusion of the dehiscent canal can be associated with vestibular dysfunction or complete vestibular loss postoperatively. In this regard, assessing the extent of the initial repair using high resolution heavily weighted T2 MRI sequences and co-registration with CT images, can guide the surgical approach and avoid unnecessary occlusion.

Limitations

Our study has several limitations: 1) the number of patients is small and further studies are needed with a greater number of revision cases. 2) Combining CT and MRI imaging requires manual co-registration. These two images have to be aligned to assess the occurrence of a persistence of fluid signal from the MRI in relation to the bony dehiscence seen on CT. To improve the alignment of the imaging, we performed a landmark registration of the MRI and CT images. However, slight misalignments may have occurred. 3) T2 signal of the SSC was segmented and transformed into a 3D model and the surrounding temporal bone was volume rendered. In the process of volume rendering, a threshold is chosen to distinguish the bone and the surrounding tissue. An effect of the chosen threshold value to determine the size of the defect cannot be excluded. 4) The results of the blinded analysis were not consistent between two observers, indicating that MRI/CT measurements can vary greatly and the 3D reconstruction images can be interpreted differently and this is likely due to the limitations of current imaging technology. Furthermore, some of the control patients had a residual defect on 3D reconstruction although they had resolution of all symptoms following primary repair, suggesting challenges with this approach, and underscores the importance of combining 2D, 3D, and clinical measures when making final recommendations to the SCD patient.

CONCLUSION

Postoperative high resolution heavily T2-weighted MRI sequences of the temporal bone can determine the extent of the SSC occlusion following primary SCD repair. Although there are several limitations to this technique, co-registration of 3D CT and MRI reconstruction of the superior canal can help determine the location of a residual defect. A detailed imaging assessment of any residual defect of the SCD repair site after primary repair provides important data for patient counseling that combined with clinical presentation may prevent unnecessary plugging that could compromise function of the ampulla or common crus.

TABLE 5. *Arc length measurements of the fluid void on postoperative MRI, the bony defect on preoperative CT, and 3D reconstruction of co-registration of CT/MRI*

Analysis No. 2								
ID	MRI Ant	MRI Post	CT Ant	CT Post	Anterior Limb	Posterior Limb	3D Ant	3D Post
Study group								
1	74	32	33	44	Plugged	**Defect**		
2	79	21	58	0	Plugged	Plugged	Plugged	**Defect**
3	58	89	46	41	Plugged	Plugged	Plugged	Plugged
4	36	51	29	58	Plugged	**Defect**	Plugged	**Defect**
5	21	29	22	37	Plugged	**Defect**	**Defect**	**Defect**
6	62	99	27	41	Plugged	Plugged	N/A	N/A
7	22	19	33	7	**Defect**	Plugged	**Defect**	**Defect**
8	36	48	N/A	N/A			**Defect**	**Defect**
9	63	45	25	31	Plugged	Plugged	Plugged	Plugged
Control group								
10	47	37	40	21	Plugged	Plugged	**Defect**	Plugged
11	55	58	23	33	Plugged	Plugged	Plugged	Plugged
12	30	73	21	49	Plugged	Plugged	Plugged	Plugged
13	64	105	25	31	Plugged	Plugged	Plugged	Plugged

A fluid void (indicating occlusion of the SSC) following primary repair was seen in all 13 cases. A total of 4/8 patients in the study group and 0/4 patients in the control group had a residual defect when comparing the fluid void with the bony defect on the preoperative CT. The 3D reconstruction suggested a residual defect in five of seven patients in the study group and one of four patients in the control group. CT indicates computed tomography; MRI, magnetic resonance imaging.

REFERENCES

1. Minor LB, Solomon D, Zinreich JS, Zee DS. Sound- and/or pressure-induced vertigo due to bone dehiscence of the superior semicircular canal. *Arch Otolaryngol Neck Surg* 1998;124:249.
2. Alkhafaji MS, Varma S, Pross SE, et al. Long-term patient-reported outcomes after surgery for superior canal dehiscence syndrome. *Otol Neurotol* 2017;38:1319–26.
3. Sharon JD, Pross SE, Ward BK, Carey JP. Revision surgery for superior canal dehiscence syndrome. *Otol Neurotol* 2016;37: 1096–103.
4. Xie Y, Sharon JD, Pross SE, et al. Surgical complications from superior canal dehiscence syndrome repair: two decades of experience. *Otolaryngol Head Neck Surg* 2017;157:273–80.
5. Ward BK, Carey JP, Minor LB. Superior canal dehiscence syndrome: lessons from the first 20 years. *Front Neurol* 2017;8:177.
6. Lookabaugh S, Kelly HR, Carter MS, et al. Radiologic classification of superior canal dehiscence: implications for surgical repair. *Otol Neurotol* 2015;36:118–25.
7. Tavassolie TS, Penninger RT, Zuñiga MG, Minor LB, Carey JP. Multislice computed tomography in the diagnosis of superior canal dehiscence: how much error, and how to minimize it? *Otol Neurotol* 2012;33:215–22.
8. Penninger RT, Tavassolie TS, Carey JP. Cone-beam volumetric tomography for applications in the temporal bone. *Otol Neurotol* 2011;32:453–60.
9. Belden CJ, Weg N, Minor LB, Zinreich SJ. CT evaluation of bone dehiscence of the superior semicircular canal as a cause of sound- and/or pressure-induced vertigo. *Radiology* 2003;226: 337–43.
10. Curtin HD. Radiology superior semicircular canal dehiscence syndrome and multi-detector row CT. *Radiology* 2003;226: 312–4.
11. Krombach GA, Di Martino E, Martiny S, et al. Dehiscence of the superior and/or posterior semicircular canal: delineation on T2-weighted axial three-dimensional turbo spin-echo images, maximum intensity projections and volume-rendered images. *Eur Arch Otorhinolaryngol* 2006;263:111–7.
12. Debnam JM, Mahfouz YM, Ketonen L, Slopis JM, McCutcheon IE, Guha-Thakurta N. Multidetector CT with 3-dimensional volume rendering in the evaluation of the spine in patients with Neurofibromatosis type 1: a retrospective review in 73 patients. *Scoliosis* 2014;9:15.
13. Carter MS, Lookabaugh S, Lee DJ. Endoscopic-assisted repair of superior canal dehiscence syndrome. *Laryngoscope* 2014;124: 1464–8.